ON THE ROLE OF THE PAIRING MODES IN THE $(h_{9/2} \otimes 3^-)$ MULTIPLET OF ^{209}Bi ☆

P.F. BORTIGNON[1]
The Niels Bohr Institute, University of Copenhagen, Copenhagen, Denmark

R.A. BROGLIA
The Niels Bohr Institute, University of Copenhagen[2], Copenhagen, Denmark
and State University of New York at Stony Brook, Physics Department, Stony Brook, New York 11794, USA

D.R. BES[3] and R. LIOTTA
Comision de Energia Atomica, Buenos Aires, Argentina

V. PAAR
Institute Ruder Boskovic, Zagreb, Croatia, Yugoslavia

Received 26 April 1976

A unified picture of the low lying states of ^{209}Bi is attempted in terms of surface and pairing vibrations as well as particle and hole degrees of freedom.

The nucleus ^{209}Bi has been investigated by means of high resolution inelastic scattering [1–4], Coulomb excitation [5, 6] and resonance fluorescence measurements [7]. Through these experiments a septuplet of states around 2.6 MeV of excitation was identified, with spins ranging from $3/2^+$ to $15/2^+$. These states have received much attention and their main features explained [8–10] in terms of the coupling between the odd-proton moving in the $1h_{9/2}$ orbital coupled to the lowest 3^- state of ^{208}Pb, as shown in figs. 1(a)–1(d).

The nucleus ^{209}Pb which is unstable has been studied by means of the ^{207}Pb(t, p)^{209}Pb, ^{210}Pb(p, d)^{209}Pb and ^{208}Pb(d, p)^{209}Pb reactions [11–14] done also with high resolution. It was recognized [15] that in this case the description in terms of the $|j(\nu) \otimes \lambda^\pi(^{208}\mathrm{Pb}); j'\rangle$ states, $j(\nu)$ denoting a single-particle neutron orbital, was too limited to account for the variety and richness of the experimental data and that both surface and pairing multipole vibrations had to be included. The corresponding analysis [15] was carried out in the basis spanned by the state vectors $|j_1(\nu) \otimes \lambda_1^\pi(^{208}\mathrm{Pb}); j'\rangle$ ($\lambda_1 = 3, 5, 2$ and $\pi = (-1)^\lambda$) and $|j_2^{-1}(\nu) \otimes \lambda_2^+(^{210}\mathrm{Pb}); j'\rangle$ ($\lambda_2 = 0, 2, 3, 6$ and 8). Good agreement was found with the experiment. To be noted is that the $15/2^-$ member of the $|1g_{9/2}(\nu) \otimes 3^-(^{208}\mathrm{Pb}); j'\rangle$ multiplet was observed in the ^{207}Pb(t, p)^{209}Pb reaction with an intensity of ≈ 0.4 of the intensity with which the lowest 8^+ state (1.271 MeV) was excited in the ^{208}Pb(t, p)^{210}Pb reaction. Also the $7/2^-$, $5/2^-$ and $3/2^-$ members of the same multiplet were observed with relatively large spectroscopic factors in the ^{210}Pb(p, d)^{209}Pb reaction. It was found that the energy of the members of the octupole multiplet is strongly affected by the states of type $|j_2^{-1}(\nu) \otimes \lambda_2^+(^{210}\mathrm{Pb}); j'\rangle$, through the graphs (k) – (n) of fig. 1.

From the experience obtained in ^{209}Pb it seems likely that to obtain a quantitative estimate of the ^{209}Bi septuplet one should utilize as basis states

$$|\mathrm{I}\rangle = |1h_{9/2}(\pi) \otimes 3^-(^{208}\mathrm{Pb}); j\rangle, \qquad (1)$$

☆ Work supported in part by ERDA contract No. E(11–1)–3001.

[1] On leave from Universita degli Stude di Padova, Istituto di Fisica Galileo Galilei, Padova, Italy. Istituto Nazionale di Fisica Nucleare, Sezione di Padova.

[2] Permanent address.

[3] Fellow of the Consejo Nacional de Investigaciones Cientificas y Tecnicas, Argentina.

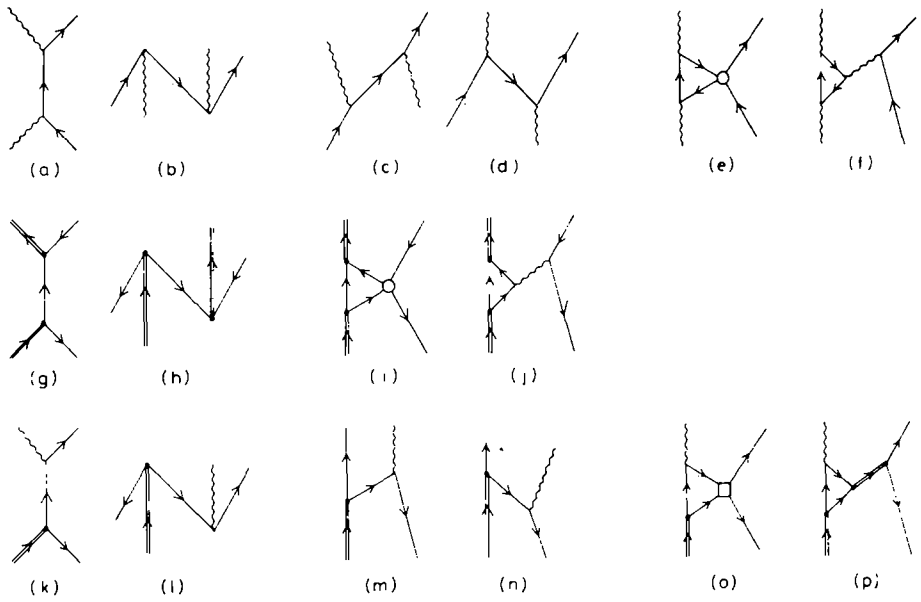

Fig. 1. All the $1/\Omega$ contributions to the energy matrix elements of the effective Hamiltonian, in the basis spanned by the vectors (1), (2). The time is assumed to run upwards. An arrowed line represents the fermion fields, while a double arrowed line and a wavy line represent the pairing and surface vibration boson. An open circle or an open square stands for the bare particle-hole and pairing multipole interaction (four-point vertices), respectively.

and

$$|\mathrm{II}\rangle = |j^{-1}(\pi) \otimes \lambda^{\pi}(^{210}\mathrm{Po}); j\rangle. \qquad (2)$$

Thus, the multipole surface and pairing vibrations and pairing vibrations and the particle and hole proton states around ^{208}Pb are utilized as building blocks to construct the ^{209}Bi spectrum ‡. This is carried out below in the framework of the nuclear field theory [16–18].

The particle-vibration coupling strength and the energy completely determine the properties of the free fields. In the case of the pairing fields, a multipole pairing force [15] with constant matrix elements was diagonalized (RPA) adjusting the coupling strengths to reproduce the experimental energies. The particles and holes (ground state correlations) were allowed to move in the $N = 2-10$ shells in the case of neutrons and in the $N = 1-9$ shells in the case of protons, N being the harmonic oscillator principal quantum number. The Coulomb correction to the energy of the valence particles was included. Its magnitude was fixed from the energy difference between the unperturbed energy of the state $|s_{1/2}^{-1}(\pi) \otimes \mathrm{gs}(^{210}\mathrm{Po}; 1/2^{+}\rangle$ ($E = 3.053$ MeV) and the energy of the state excited in the ^{210}Po(t, α) reaction [19] with $l = 0$ with spectroscopic factor $S \approx 2$ ($E = 2.43$ MeV). The resulting value is $E_c \approx 300$ keV.

In the case of the surface phonons a multipole particle-hole interaction containing both isoscalar and isovector components was diagonalized. Excitations of $\Delta N = 0$ and $\Delta N = 2$ type were allowed for $\lambda^{\pi} = 2^{+}$ and $\Delta N = 1$ and $\Delta N = 3$ for $\lambda^{\pi} = 3^{-}$. The selfconsistent values of $\kappa(\tau, \lambda)$ were utilized for $\lambda = 2$ (cf. ref. [20]; see also ref. [21]), and all the resulting phonons were allowed as intermediate states in the matrix elements of fig. 1. For the $\lambda = 3$ mode, κ ($\tau = 0$, $\lambda = 3$) was adjusted to reproduce the experimental energy (2.615 MeV) of the lowest octupole mode, setting the ratio κ ($\tau = 0$, $\lambda = 3$)/κ ($\tau = 1$, $\lambda = 3$) equal to -4.6 (cf. eq. (3.5) of ref. [21]). The resulting value of the isoscalar strength is $(91/A^2)(M\omega/\hbar)^3$ MeV.

The energies of the fermion fields, i.e., the energies of the proton particle and hole states $j(\pi) = (1h_{9/2},$

‡ A preliminary account of this approach was reported in [19]. See also ref. [10].

$2f_{7/2}$, $1i_{13/2}$, $3p_{3/2}$, $2f_{5/2}$, $3p_{1/2}$, $1i_{11/2}$) and $j^{-1}(\pi) = (3s_{1/2}, 2d_{3/2}, 1h_{11/2}, 2d_{5/2}, 1g_{9/2})$ were taken from experiment.

Utilizing the calculated particle-vibration and four-point vertices coupling strengths and the corresponding free field energies, the effective matrix elements displayed in fig. 1 were worked out. As discussed in [18], the small parameter upon which to expand in the nuclear field theory is $1/\Omega$, where $\Omega = \Sigma_j(j+1/2)$ is the effective degeneracy of the valence shells. Because the particle-vibration vertices are of order $1/\sqrt{\Omega}$ and the four-point vertices are of order $1/\Omega$ (cf. ref. [17]), while a closed loop contributes a factor Ω, the graphs displayed in fig. 1 constitute all the $1/\Omega$ (lowest order) contributions to the energy. The energy denominators of each graph contains products of differences between the exact energy and the energy of the intermediate states. There is thus one matrix for each state which has to be diagonalized selfconsistently. The resulting energies and wavefunctions for all the states of type (1)–(2) which are strongly excited in any of the reactions

$$^{209}\mathrm{Bi}\,(\mathrm{d}, \mathrm{d}')^{209}\mathrm{Bi}, \qquad ^{210}\mathrm{Po}\,(\mathrm{t}, \alpha)^{209}\mathrm{Bi}, \qquad (3)$$

and

$$^{208}\mathrm{Pb}\,(^{3}\mathrm{He}, \mathrm{d})^{209}\mathrm{Bi},$$

are displayed in table 1. Note that the square of the amplitudes of each state sums to a number different from one (also shown in table 1). In fact, the normalization of each state corrects for the overcompleteness of the basis (1) and (2) (cf. ref. [22]).

Utilizing the amplitudes of table 1 we have graphically calculated the inelastic transition probabilities and the one proton pick-up and stripping spectroscopic factors, again to lowest order in the parameter $1/\Omega$. The corresponding results are displayed in table 1 in comparison with the experimental values associated with the reactions (3).

The interplay between states of type (1) and (2) in the physical states is particularly illustrated in the case of the two $3/2^+$ states. These states start at an unperturbed energy of 2.615 MeV (corresponding to the $|1h_{9/2} \otimes 3^-\ (^{208}\mathrm{Pb}); 3/2^+\rangle$ component) and 2.733 MeV (corresponding to the $|2d_{3/2}^{-1} \otimes \mathrm{gs}\ (^{210}\mathrm{Po}); 3/2^+\rangle$ component). The matrix elements between them are

Table 1

States strongly excited in one or more of the reactions $^{208}\mathrm{Pb}(^{3}\mathrm{He}, \mathrm{d})^{209}\mathrm{Bi}$, $^{210}\mathrm{Po}\,(\mathrm{t}, \alpha)^{209}\mathrm{Bi}$ and $^{209}\mathrm{Bi}(\mathrm{d}, \mathrm{d}')^{209}\mathrm{Bi}(J^\pi)$. In the first and second column the spin and parity and the energy of the states is given. In column 3 the main component of the wavefunctions in terms of the basis states (cf. eqs. (1) and (2)) are collected. The number in parentheses at the end of each wavefunction is equal to the square root of the sum of the amplitudes squared. In the fourth and fifth columns we give the experimental and theoretical energy difference $E_j = (E_j - 2615)$ keV of the members of the septuplet measured with respect to the energy of the 3^- state in $^{208}\mathrm{Pb}$. For the second state $3/2^+$(2.95 MeV) and for the $1/2^+$(2.43 MeV) and $11/2^-$(3.69 MeV) we give instead the absolute excitation energy. In columns 6 and 7 we collect the experimental and theoretical inelastic excitation cross section normalized to the $3^-(^{208}\mathrm{Pb})$ cross section according to $\frac{\mathrm{d}\sigma(\mathrm{h}_{9/2}(^{209}\mathrm{Bi}) \to J(^{209}\mathrm{Bi}))}{\mathrm{d}\sigma(\mathrm{gs}(^{208}\mathrm{Pb}) \to 3^-(^{208}\mathrm{Pb}))}$ (%). A polarization charge of 0.3 for protons and 0.8 for neutrons (cf. ref. [20]) was utilized in the theoretical estimates to account for the effects of high lying octupole states. In the columns 8 and 9 the experimental and theoretical values of the (t, α) spectroscopic factor are displayed. In the two final columns we give the spectroscopic factors associated with the (^{3}He, d) reaction.

$$M^{(\mathrm{m})}(E) = \begin{cases} 319\ \mathrm{keV}\ (E = 2.479\ \mathrm{MeV}) \\ 482\ \mathrm{keV}\ (E = 3.075\ \mathrm{MeV}) \end{cases}$$

(graph (m) of fig. 1),

and

$$M^{(\ell)}(E) = \begin{cases} -93\ \mathrm{keV}\ (E = 2.479\ \mathrm{MeV}) \\ -102\ \mathrm{keV}\ (E = 3.075\ \mathrm{MeV}) \end{cases}$$

(graph (ℓ) of fig. 1).

The energy dependence of $M^{(\mathrm{m})}$ and $M^{(\ell)}$ is again related to the overcompleteness of the basis (1), (2). The main consequence of including states of both types (1) and (2), and to treat its interaction according to the nuclear field theory rules, is evidenced in the very different ratio of the (d, d') and (t, α) cross sections associated with the two $3/2^+$ states. While $R_1 = B(\mathrm{E3}; (3/2)_1)/B(\mathrm{E3}; (3/2)_2)$ is approximately equal to 4, the ratio $R_2 = \sigma((\mathrm{t}, \alpha); (3/2)_1)/\sigma((\mathrm{t}, \alpha); (3/2)_2)$ is close to one. Noting that the component of type (1) carries basically all the inelastic strength while the (t, α) proceeds through the component of type (2), a treatment which neglects the overcompleteness of the basis predicts $R_2 = 1/R_1$.

	E(MeV)		t_E		B(E3)	(%)	S(t,0)		S(^{3}He,d)	
J^π	exp[a]	wavefunction	exp[a]	th	exp[a]	th	exp[b]	th	exp[c]	th
$3/2^+$	2.494	$-0.53\|d^{-1}_{3/2} \otimes 0^+\rangle$ $-0.03\|d^{-1}_{3/2} \otimes 2^+\rangle$ $0.02\|f_{7/2} \otimes 3^-\rangle$ $0.76\|h_{9/2} \otimes 3^-\rangle$ (0.928)	-121	-136	4.2±0.3	3.7	1.8±0.3	1.81	< 0.01	0.02
$5/2^+$	2.618	$0.02\|d^{-1}_{5/2} \otimes 0^+\rangle$ $-0.06\|d^{-1}_{3/2} \otimes 2^+\rangle$ $-0.01\|d^{-1}_{3/2} \otimes 4^+\rangle$ $0.07\|f_{7/2} \otimes 3^-\rangle$ $0.98\|h_{9/2} \otimes 3^-\rangle$ (0.983)	3	- 46	9.1±0.5	8.6				
$7/2^+$	2.585	$-0.05\|d^{-1}_{3/2} \otimes 2^+\rangle$ $-0.02\|d^{-1}_{3/2} \otimes 4^+\rangle$ $-0.02\|s^{-1}_{1/2} \otimes 4^+\rangle$ $-0.04\|f_{7/2} \otimes 3^-\rangle$ $1.00\|h_{9/2} \otimes 3^-\rangle$ (1.005)	- 30	30	12.3±0.5	11				
$9/2^+$	2.566	$-0.01\|d^{-1}_{3/2} \otimes 4^+\rangle$ $0.02\|f_{7/2} \otimes 3^-\rangle$ $0.96\|h_{9/2} \otimes 3^-\rangle$ (0.985)	- 49	- 90	13.8±0.6	15.8				
$11/2^+$	2.600	$-0.03\|d^{-1}_{3/2} \otimes 4^+\rangle$ $-0.02\|f_{7/2} \otimes 3^-\rangle$ $1.02\|h_{9/2} \otimes 3^-\rangle$ (1.018)	- 15	- 20	37.4±(0.7)[d]	18.5			0.06	0.03
$13/2^+$	2.600	$0.09\|f_{7/2} \otimes 3^-\rangle$ $0.96\|h_{9/2} \otimes 3^-\rangle$ (0.965)	- 15	- 80		20.7				0.01
$15/2^+$	2.744	$1.08\|h_{9/2} \otimes 3^-\rangle$ (1.081)	129	190	23.7±0.7	20.0	≲ 0.2		< 0.02	0.01
$3/2^+$	2.95	$-0.92\|d^{-1}_{3/2} \otimes 0^+\rangle$ $0.18\|d^{-1}_{3/2} \otimes 2^+\rangle$ $0.14\|s^{-1}_{1/2} \otimes 2^+\rangle$ $0.17\|f_{7/2} \otimes 3^-\rangle$ $-0.71\|h_{9/2} \otimes 3^-\rangle$ (1.195)	3.075 MeV		1.1±(0.2)[d]	1.3	2.2±0.3	1.96	< 0.01	
$1/2^+$	2.43	$-0.99\|s^{-1}_{1/2} \otimes 0^+\rangle$ $0.11\|f_{7/2} \otimes 3^-\rangle$	2.5 MeV				1.8	1.94	< 0.02	0.02
$11/2^-$	3.69	$0.99\|h^{-1}_{11/2} \otimes 0^+\rangle$ $0.07\|i_{13/2} \otimes 3^-\rangle$	3.76 MeV				10	11.86	< 0.05	0.01

a) Ref. 2
b) Ref. 19
c) Ref. 23
d) Error estimated (not given in original reference).

The largest coupling between the main components (1) and (2) of the two $3/2^+$ states is due to the graph (m) of fig. 1. However, the contribution of the graph (ℓ) of fig. 1 and the corresponding contributions to the (d, d′) process amount to ~ 30% of the previous contribution.

A consistent picture of the low-lying levels of ^{209}Bi can be obtained in the framework of the nuclear field theory in terms of pairing and surface vibrations and single-particle and hole degrees of freedom.

Discussions with A. Bohr and B.R. Mottelson are gratefully acknowledged.

References

[1] J.C. Hafele and R. Woods, Phys. Lett. 23 (1966) 579.
[2] J. Ungrin, R.M. Diamond, P.O. Tjøm and B. Elbek, Kong. Dan. Vid. Selsk. Mat. Fys. Medd. 38 (1971) no. 9.
[2] S. Hinds, H. Marchant, J.H. Bjerregaard and O. Nathan, Phys. Lett. 20 (1966) 674.
[4] T.P. Cleary et al., Phys. Rev. Lett. 28 (1972) 699.
[5] R.A. Broglia, J.S. Lilley, R. Perazzo and W.R. Phillips, Phys. Rev. C1 (1970) 1508.
[6] J.W. Hertel, D.G. Fleming, J.P. Schiffer and H.E. Gove, Phys. Rev. Lett. 23 (1969) 488.
[7] F.R. Metzger, Phys. Rev. B187 (1969) 1680.
[8] B.R. Mottelson, J. Phys. Soc. Japan Suppl. 24 (1968) 87.
[9] R.A. Broglia, J. Damgaard and A. Molinari, Nucl. Phys. A127 (1969) 429.
[10] I. Hamamoto, Nucl. Phys. A126 (1969) 545, Nucl. Phys. A126 (1969) 545, Nucl. Phys. A135 (1969) 576; A141 (1970) 1; Phys. Rep. 10C (1974) 63.
[11] E.R. Flynn, G. Igo, P.D. Barnes, D. Kovar, D. Bes and R.A. Broglia, Phys. Rev. C3 (1971) 2371.
[12] E.R. Flynn, G. Igo, P. Barnes and D. Kovar, Phys. Rev. Lett. 22 (1969) 142.
[13] G. Igo, P. Barnes, E. Flynn and B. Dropesky, Phys. Rev. C3 (1971) 349.
[14] D. Kovar, thesis, unpublished.
[15] D.R. Bes and R.A. Broglia, Phys. Rev. C3 (1971) 2349.
[16] D.R. Bes, G.G. Dussel, R.A. Broglia, R. Liotta and B.R. Mottelson, Phys. Lett. 52B (1974) 253.
[17] D.R. Bes, R.A. Broglia, G.G. Dussel and R. Liotta, Phys. Lett. 56B (1975) 109.
[18] D.R. Bes, R.A. Broglia, G.G. Dussel, R.J. Liotta and H.M. Sofia, Nucl. Phys., in press;
D.R. Bes, R.A. Broglia, G.G. Dussel, R.J. Liotta and R. Perazzo, Nucl. Phys., in press.
[19] P.D. Barnes et al., Nucl. Phys. A195 (1972) 146.
[20] A. Bohr and B.R. Mottelson, Nuclear structure, Vol. II (Benjamin, New York 1976).
[21] D.R. Bes, R.A. Broglia and B.S. Nilsson, Phys. Rev. 16C (1975) 1.
[22] D.R. Bes, R.A. Broglia, G.G. Dussel, R.J. Liotta and B.R. Mottelson, to be published.
[23] B. Wildenthal, B. Preedom, E. Newman and M. Cates, Phys. Rev. Lett. 19 (1967) 960;
C. Ellegaard and P. Vedelsby, Phys. Lett. 26B (1968) 155.